 doi:10.20944/preprints202009.0238.v1

Tumoral HLA class I and APM expression and its effect on intratumoral T-cell reaction and outcome in HPV-negative oral squamous cell carcinoma

Short running title: Tumor microenvironment and HLA-I expression in HPV-negative OSCC

Claudia Wickenhauser[1#], Daniel Bethmann[1#], Matthias Kappler[2#], Alexander W. Eckert[2], André Steven[3], Jürgen Bukur[3], Bernard A. Fox[4], Jana Beer[1] and Barbara Seliger[3]

Affiliations:

[1] University Hospital Halle (Saale), Institute of Pathology, Halle (Saale), Germany

[2] University Hospital Halle (Saale), Department of Oral and Maxillofacial Plastic Surgery, Halle (Saale), Germany

[3] University Hospital Halle (Saale), Institute of Medical Immunology, Halle (Saale), Germany

[4] Robert W. Franz Cancer Research Center, Earle A. Chiles Research Institute, Portland, Oregon, USA

# These authors contributed equally to this work.

Corresponding author: Prof. Dr. Barbara Seliger
Martin Luther University Halle-Wittenberg
Institute of Medical Immunology
Magdeburger Str. 2
06112 Halle (Saale)
Germany

Telephone: +49 (0) 345 557 4054

Fax: +49 (0) 345 557 4055

E-mail: barbara.seliger@uk-halle.de

 doi:10.20944/preprints202009.0238.v1

List of abbreviations

ALAS 1, delta-aminolevulinate synthase 1; APM, antigen processing machinery; β_2-m, beta-2-microglobulin; CPI, checkpoint inhibitor; CRC, colorectal cancer; CSI, cumulative suppression index; CTL, cytotoxic T lymphocyte; DAB, 3,3'-diaminobenzidine; FFPE, formalin-fixed paraffin-embedded; FITC, fluorescein isothiocyanate; FoxP3, Fork head-Box-Protein P3; GAPDH, glyceraldehyde-3-phosphate dehydrogenase; HC, heavy chain; HLA, human leukocyte antigen; HLA-I, human leukocyte antigen class I; HNC, head and neck cancer; HNSCC, head and neck squamous cell carcinoma; HPV, human papilloma virus; HRP, horseradish peroxidase; IFN, interferon; IHC, immunohistochemistry; IM, invasive margin; IRS, international rating score; LMP, low molecular weight protein; mAb, monoclonal antibody; MFI, mean specific fluorescence intensity; MSI, multispectral imaging; OS, overall survival; OSCC, oral squamous cell carcinoma; PBMC, peripheral blood mononuclear cells; PCR, polymerase chain reaction; PD-L1, programmed death-like receptor ligand 1; ROC curves, Receiver-Operating-Characteristic curves; RR, relative risk; RT, room temperature; STAT, signal transducer and activator of transcription; TA, tumor antigen; TAM, tumor associated macrophages; TAP, transporter associated with antigen processing; TC, tumor center; TCGA, The Cancer Genome Atlas; TIL, tumor infiltrating lymphocyte; TME, tumor microenvironment; tpn, tapasin; Treg, regulatory T cell; TSA, tyramide signal amplification; UICC, Union Internationale Contre le Cancer.

Preprints (www.preprints.org) | NOT PEER-REVIEWED | Posted: 10 September 2020 doi:10.20944/preprints202009.0238.v1

Abstract

Progression of oral squamous cell carcinoma (OSCC) has been associated with an escape of tumor cells from the host immune surveillance with growing evidence of its underlying molecular mechanisms and its interaction with the immune cell control. In this study the expression of HLA class I (HLA-I) antigens and of components of the antigen processing machinery (APM) was analyzed in 160 consecutive human papilloma virus (HPV)-negative OSCC lesions and correlated to tumor specific parameters, the intratumoral immune cell response and to the patients outcome. A heterogeneous, but predominantly lower constitutive protein expression of HLA-I APM components was seen in OSCC sections when compared to non-neoplastic cells. Based on the expression levels of HLA-I APM components three main OSCC subgroups were detected and categorized into HLA-I^{high}/APM^{high}, HLA-I^{low}/APM^{low} and HLA-$I^{discordant\ high/low}$/APM^{high} phenotypes. In the HLA-I^{high}/APM^{high} group, the highest frequency of intratumoral $CD8^+$ T cells and lowest number of $CD8^+$ T cells close to FoxP3 cells was found. Despite being associated with the highest T cell infiltration, patients within this group presented the most unfavorable survival, which was most evident in stage T2 tumors. Thus, the presented findings strongly indicate the presence of additional factors involved in the immunomodulatory process of HPV-negative OSCC with a possible tumor-burden-dependent complex network of immune escape mechanisms beyond HLA-I/APM components and T cell infiltration in this tumor entity.

Key words: oral squamous cell carcinoma, HLA class I, antigen processing machinery, immune cell infiltration, immune escape, prognosis

Preprints (www.preprints.org) | NOT PEER-REVIEWED | Posted: 10 September 2020 doi:10.20944/preprints202009.0238.v1

1. Introduction

As one of the eight “hallmarks of cancer”, the interaction between immune- and tumor cells plays an integral role in controlling the initiation and progression of malignant diseases. A growing body of evidence of changes in the expression of immune modulatory molecules on tumor cells and on cells of the tumor microenvironment (TME) as well as of alterations in the immune contexture, in particular the nature, composition, density, localization, and function of immune cell subpopulations, soluble and physical factors, continuously leads to a better understanding of the tumor immune surveillance and immune escape [1]. The characterization of these mechanisms will give insights into the development of innate and acquired resistances to immunotherapies [2, 3], which is crucial for improving the efficacy of immunotherapies for the treatment of cancer patients [4, 5].

In murine experimental models as well as in human malignant tumors a number of immune escape strategies, resulting in T cell tolerance and loss of T cell recognition, has been described. These include (i) lack or downregulation of tumor antigen expression, (ii) loss or reduced expression of HLA-I surface molecules due to impaired expression of APM components, (iii) increased expression of immune suppressive molecules, e.g. the programmed death-like receptor ligand 1 (PD-L1) and the non-classical HLA-G and HLA-E antigens, (iv) downregulation of the interferon (IFN) signal pathways, (v) activation of oncogenic signaling and (vi) alterations in the expression of inflammatory cytokines, metabolites and pH as well as (vii) transcription factors [6-9]. Despite a loss of heterozygosity and somatic mutations of HLA-I antigens have been described in different tumor entities [10-12], their frequency is relatively rare suggesting that the impaired HLA-I surface expression of tumors appears to be mainly due to a deregulation of HLA-I APM components, such as the transporter associated with antigen processing (TAP) subunits and low molecular weight proteins (LMPs), mediated by epigenetic, transcriptional and/or post-transcriptional control [9, 13]. This can occur at each step of the complex HLA-I APM and affect the anti-tumoral T cell responses [14-17]. Furthermore, an immune suppressive TME mediated by e.g. cellular and soluble components as well as by the interaction of the intra- and peritumoral immune cells negatively interferes with the immune control and could influence the prognosis of tumor patients and their response to (immuno)therapies [14, 18].

Despite recent treatment advances, oral squamous cell cancer (OSCC) is with 700.000 new cases and 380.000 deaths worldwide [19] still one of the leading causes of cancer worldwide with an overall poor prognosis [20, 21]. In industrialized countries, it is mainly attributed to smoking and alcohol abuse and is in about 5% of cases associated with human papilloma virus (HPV) infection [22]. Early disease is treated by either surgery or radiotherapy, while for recurrent/metastatic disease palliative chemotherapy is currently the standard of care [23]. Despite advances in cytotoxic therapies and surgical intervention, the prognosis of patients is

Preprints (www.preprints.org) | NOT PEER-REVIEWED | Posted: 10 September 2020 doi:10.20944/preprints202009.0238.v1

still limited with only little improvement of their outcome over the last decades [24]. Cancer immunotherapies, in particular immune checkpoint inhibitors (CPI), have been shown to increase the overall survival (OS) of OSCC patients, which led to the FDA approval of the anti-PD-L1 antibody Nivolumab for their treatment [25, 26]. Despite these promising results, only transiently responses or durable responses in a limited number of patients are generated, while the majority of OSCC patients progress and die of their disease [27]. Thus, there is an urgent need to identify prognostic and predictive markers and novel therapeutic targets. Emerging evidence of an enriched immune landscape with key immunological features and prognostic relevance in OSCC exists, which was confirmed by *in silico* analyses of TCGA data [28]. In colorectal cancer (CRC) the quantification of adaptive immune cells composed of $CD3^+$ T lymphocytes with a cytotoxic (CD8) and memory (CD45RO) phenotype located at the invasive margin (IM) and tumor center (TC) called “immunoscore” was established as a risk predictor more powerful than TNM and histologic grading in this context. The use of the “immunoscore” as a consensus biomarker [29, 30] and as a tool to distinguish between responders and non-responders to CPI therapies [31] might be also useful for OSCC patients.

Concerning HPV^- OSCC, our group recently proposed a more sophisticated immunoscore termed “cumulative suppression index” (CSI). By evaluating the density and geography of the TME, in particular the spatial distance of $CD3^+/CD8^+$ T cells to $CD3^+/CD8^-/FoxP3^+$ T cells, the CSI was of prognostic relevance in large tumors independent of well-established prognostic factors and it had a strong effect on the patient’s OS [32]. However, OSCC cells have developed different strategies to counteract immune recognition involving both intrinsic cancer related factors and extrinsic mechanisms, like an immune suppressive TME and the downregulated expression of HLA-I APM surface antigen components recognized by tumor-specific T cells due to the reduced expression of HLA-I APM components [6]. Mapping these escape mechanisms might help to develop strategies to overcome this tolerance [33]. Therefore, the expression of HLA-I HC, β_2-m and four distinct APM components (TAP1, TAP2, LMP2 and LMP10) was determined in 160 HPV^- OSCC using immunohistochemistry (IHC) and qPCR, respectively. These data were correlated to tumor specific characteristics, the composition of the TME and the patients’ outcome and were further validated by evaluation of corresponding data of The Cancer Genome Atlas (TCGA) from 103 HPV^- HNSCC cases.

Preprints (www.preprints.org) | NOT PEER-REVIEWED | Posted: 10 September 2020 doi:10.20944/preprints202009.0238.v1

2. Results

2.1 Clinicopathologic data

A comprehensive overview of the clinicopathologic data and the OS of the 160 HPV$^-$ OSCC patients included in this study is provided in Table 1A. Gender and age had no influence on the survival, while the T stage and the presence of metastases significantly correlated with a poor survival. These data were confirmed by TCGA cohort analysis of 103 HPV$^-$ HNC, where no prognostic differences concerning gender and age of the patients were reported. Instead, a better survival was found for HPV$^-$ HNC patients at low N stage. Unexpected, but in line with other studies, the WHO tumor grading had no prognostic significance in both collectives (Table 1A) [34].

In Table 1B, information concerning therapy regimen is provided demonstrating that locally extended tumors received radiation therapy, while adjuvant standard chemotherapy was administered in all cases with tumor dissemination irrespective of tumor size, but in particular in patients with a T1/2 tumor.

Table 1: Patient specific characteristics

A: Clinicopathologic data and overall survival of 160 HPV$^-$ OSCC patients

category	no. of cases	overall survival (OS): all tumors	
		univariable analysis	multivariable analysis*
		RR; p-value	RR; p-value
gender			
men	124		
women	36	0.79; p=0.4	0.87; p=0.64
age (years)			
≤ 60	91		
> 60	69	1.17; p=0.49	1.29; p=0.26
T stage			
I	32		
II	49	**2.54; p=0.025**	**2.75; p=0.02**
III	24	**3.04; p=0.018**	**3.10; p=0.028**
IV	55	**6.99; p<0.0001**	**6.92; p<0.0001**
N stage			
N0	71		
N1-3	89	**2.22; p=0.001**	1.26; p=0.4
M stage			
M0	154		
M1	6	2.41; p=0.057	**3.16; p=0.017**
grading			
1	18		

Preprints (www.preprints.org) | NOT PEER-REVIEWED | Posted: 10 September 2020 doi:10.20944/preprints202009.0238.v1

2 3	107 35	0.96; p=0.92 0.85; p=0.69	0.65; p=0.24 0.58; p=0.2

*Cox proportional hazards regression: adjusted for T, N stage and grading; RR, relative risk. Statistically significant data is marked in bold.

B: Frequency and intensity of adjuvant therapy

UICC T stage	number of cases	adjuvant radiation therapy received	median dosage (gy)	adjuvant standard chemotherapy received
I	32	14 (44%)	50,2	24 (75%)
II	49	26 (53%)	50,0	12 (25%)
III	24	17 (71%)	64,0	9 (38%)
IV	55	40 (73%)	64,0	31 (56%)

The frequency of radiation therapy (%) including the median dosage as well as the frequency of standard chemotherapy (%) of patients in different T stages is given.

2.2 HLA-I/APM expression in OSCC tumors

In order to determine the expression levels of HLA-I/APM components in OSCC, protein expression of HLA-I HC, β_2-m and the APM molecules TAP1, TAP2, LMP2 and LMP10 were analyzed by IHC of formalin-fixed, paraffin embedded (FFPE) tumor lesions [35]. IHC staining revealed at least slightly reduced, but heterogeneous cytoplasmic, membranous and / or nuclear expression levels depending on HLA-I and APM components analyzed when compared to the surrounding non-malignant cells (data not shown).

Based on the HLA-I (HC/β_2-m) and APM (TAP, LMP) component expression pattern in the FFPE lesions, OSCC were categorized into four distinct HLA/APM phenotypes (phenotype I-IV, see Materials and Methods). In short, while phenotype I expressed high levels of both the HLA-I HC/β_2-m and APM components (**HLA-I^{high}/APM^{high}**), phenotype II displayed a concordant low expression pattern of HC/ β_2-m and APM component (**HLA-I^{low}/APM^{low}**). Phenotype III expressed discordant levels of HLA-I HC/β_2-m and high levels of APM components (**HLA-I$^{discordant\ high/low}$/APM^{high}**). Phenotype IV with discordant HLA-I and low APM expression was omitted from further analyses due to low the group size (Table 2A). It is noteworthy that the three HLA/APM phenotypes were uniformly distributed over the different T stages (Table 2B). As the HC10 antibody only recognizes the HLA-I HC, corresponding fresh frozen OSCC tissues from five FFPE OSCC lesions with phenotype I and five OSCC lesions with phenotype II were stained with the HLA-A/B/C antibody W6/32 recognizing the functional trimeric HLA-I HC/β_2-m and peptide complex [36]. In these selected cases, the expression levels of HLA-I HC together with β_2-m staining were comparable to those obtained by employing the W6/32 monoclonal antibody (mAb). These findings suggest expression of the

Preprints (www.preprints.org) | NOT PEER-REVIEWED | Posted: 10 September 2020 doi:10.20944/preprints202009.0238.v1

functional trimeric HLA-I complex at least in the OSCC cases analyzed (Figure 1, Supplementary Table 1). As a further control, HLA-I HC and ß$_2$-m mRNA expression was analyzed in a subset of OSCC specimen also demonstrating concordant expression profiles when compared to the protein data (data not shown).

Table 2: HLA-I and APM protein expression patterns in OSCC lesions

A: Classification of OSCC lesions according to the HLA-I/APM expression

HLA-I/APM phenotype	patients (n=160)	HC	β$_2$-m	TAP1	TAP2	LMP2	LMP10	expression pattern
I [HLA-I^{high} – APM^{high}]	57 (36%)	+	+	+	+	+	+	concordant HLA-I/APM expression
II [HLA-I^{low} – APM^{low}]	12 (8%)	-	-	-	-	-	-	
III [HLA-I$^{discordant\ high/low}$ - APM^{high}]	89 (56%)	+	-	+	+	+	+	discordant HLA-I/APM expression
		-	+					
IV [HLA-I$^{discordant\ high/low}$ - APM^{low}]*	2 (<1%)	+	-	-	-	-	-	
		-	+					

* omitted from further analyses due to limited group size. A discordant HLA-I HC and β$_2$-m expression is marked as $^{high/low}$.

B: Distribution of T stages across HLA-I/APM phenotypes

HLA-I/APM phenotype	T1	T2	T3	T4	all Ts
I [HLA-I^{high}/ APM^{high}]	16 (50%)	15 (31%)	12 (50%)	14 (26%)	57 (36%)
II [HLA-I^{low}/ APM^{low}]	3 (9%)	2 (4%)	3 (13%)	4 (7%)	12 (8%)
III [HLA-I$^{discordant\ high/low}$/APM^{high}]	12 (38%)	31 (63%)	9 (37%)	37 (67%)	89 (55%)
IV [HLA-I$^{discordant\ high/low}$/APM^{low}]*	1 (3%)	1 (2%)	-	-	2 (1%)

* omitted from further analyses due to limited group size. A discordant HLA-I HC and β$_2$-m expression is marked as $^{high/low}$.

Preprints (www.preprints.org) | NOT PEER-REVIEWED | Posted: 10 September 2020 doi:10.20944/preprints202009.0238.v1

Figure 1: Differential expression of HLA-I HC, β_2-m and HLA-I complex in OSCC lesions

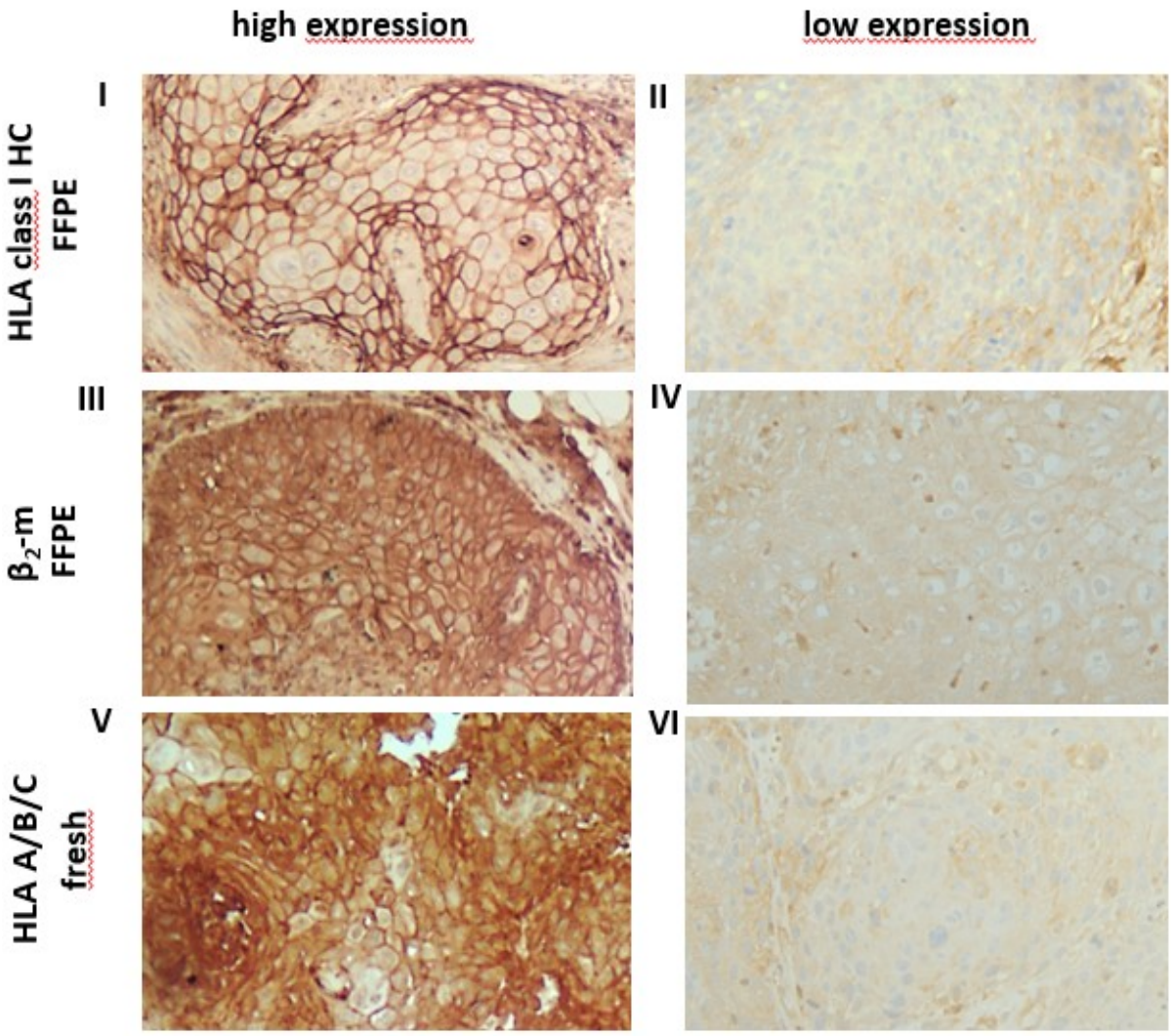

Representative immunohistochemistry using antibodies directed against HLA class I HC (FFPE, I, II), β_2-m (FFPE III, IV) and the trimeric HLA class I A/B/C complex (W6/32; fresh frozen, V, VI). Representative cases with a high (I, III) or low (II, IV) cytoplasmic and membranous expression of HLA class I HC and β_2-m in FFPE samples are shown and compared to a staining of the trimeric HLA class I complex (V, VI) on fresh frozen tissues. Each image was done at a 200x resolution.

Preprints (www.preprints.org) | NOT PEER-REVIEWED | Posted: 10 September 2020 doi:10.20944/preprints202009.0238.v1

2.3 Impact of tumoral HLA-I/APM expression on the intratumoral immune cell reaction

To elucidate the impact of OSCC HLA-I/APM expression on the immune cell repertoire, the HLA-I HC and/or β_2-m expression data was correlated to the frequency and composition of intratumoral T cell subsets recently acquired by multispectral imaging within the same sample collective [32]. In this approach, the intensity of tumoral HLA-I HC/β_2-m surface expression correlated highly significant positively with the density of intratumoral $CD8^+$ T cells (p=0.008 resp. 0.003), but negatively with the number of $CD8^+$ T cells adjacent to $FoxP3^+$ cells within a radius of 30 µm (p=0.009 resp. 0.007) (Table 3A). Furthermore, a positive correlation between the expression of LMP2 and the density of $CD8^+$ T cells was detected (p=0.003). A similar distribution of the intratumoral T cell subsets was detected within the different tumor stages (Table 3B).

In silico analyses of TCGA data were in line with these findings as the mRNA expression levels of all HLA-I/APM genes were correlated positively with the quantity of the T cell infiltrate, in particular demonstrating a significant relation of CD8A with the HLA-I HC, β_2-m, TAP1, TAP2, LMP2 and LMP10 (Table 3C, Suppl. Figure 1).

Table 3: Correlation of tumoral HLA-I and APM component expression with the intratumoral T cell infiltrate

A: Bivariable correlation of the expression of the HLA-I HC, β_2-m and APM components with the intratumoral T cell infiltrate

intratumoral T cell infiltrate		**MHC class I HC**	**β_2-m**	**TAP1**	**TAP2**	**LMP2**	**LMP10**
	N	r_s (p-value)	r_s (p-value)	r_s (p-value)	r_s (p-value)	r_s (p-value)	r_s (p-value)
$CD4^+/mm^2$	108	0.150 (0.12)	0.216 (0.03)*	-0.142 (0.14)	0.168 (0.08)*	0.229 (0.017)*	0.120 (0.22)
$CD8^+/mm^2$	119	**0.242 (0.008)****	**0.272 (0.003)****	-0.172 (0.08)*	0.118 (0.20)	**0.270 (0.003)****	0.095 (0.30)
$FoxP3^+/mm^2$	119	0.190 (0.04)*	**0.246 (0.007)****	-0.239 (0.01)*	0.198 (0.03)*	0.146 (0.11)	0.012 (0.90)
$CD8^+$ to $FoxP3^+$ within 30 µm	119	**-0.238 (0.009)****	**-0.248 (0.007)****	-0.034 (0.73)	-0.043 (0.64)	-0.223 (0.015)*	-0.024 (0.79)

Spearman's Rho test: r_s-correlation coefficient; statistically significant data are marked in bold.

* denotes p<0.05; ** denotes p<0.01

Preprints (www.preprints.org) | NOT PEER-REVIEWED | Posted: 10 September 2020 doi:10.20944/preprints202009.0238.v1

B: Intratumoral density of T cell subpopulations across the HLA-I/APM phenotypes I-III in correlation to the T stage

HLA-I/APM phenotype	T stage	median $CD8^+/mm^2$	median $CD4^+/mm^2$	median $FoxP3^+/mm^2$
I [HLA-I^{high}-APM^{high}]	1-4	269	65	92
	1	220	59	203
	2	271	78	107
	3	262	53	90
	4	305	35	74
II [HLA-I^{low}-APM^{low}]	1-4	23	15	30
	1	30	0	15
	2	66	26	69
	3	6	3	3
	4	16	32	20
III [HLA-$I^{high/low}$-APM^{high}]	1-4	96	42	70
	1	209	90	107
	2	48	18	67
	3	69	19	34
	4	116	51	81

C: Correlation of the mRNA expression of HLA-I/APM components with T cell markers using TCGA data from HPV^- HNC patients

	HLA-A	β_2-m	TAP1	TAP2	LMP2	LMP10
CD4	$r_s = 0.351$ ($p = 2.3e^{-3}$)	$r_s = 0.458$ ($p = 4.6e^{-5}$)	$r_s = 0.394$ ($p = 5.6e^{-4}$)	$r_s = 0.372$ ($p = 1.2e^{-3}$)	$r_s = 0.328$ ($p = 4.6e^{-3}$)	$r_s = 0.474$ ($p = 2.3e^{-5}$)
CD8A	$r_s = 0.506$ ($p = 5.0e^{-6}$)	$r_s = 0.698$ ($p = 7.0e^{-12}$)	$r_s = 0.699$ ($p = 1.5e^{-11}$)	$r_s = 0.642$ ($p = 9.4e^{-10}$)	$r_s = 0.653$ ($p = 3.7e^{-10}$)	$r_s = 0.671$ ($p = 7.9e^{-11}$)
FoxP3	$r_s = 0.347$ ($p = 2.7e^{-3}$)	$r_s = 0.460$ ($p = 4.2e^{-5}$)	$r_s = 0.445$ ($p = 7.9e^{-5}$)	$r_s = 0.45$ ($p = 6.4e^{-5}$)	$r_s = 0.342$ ($p = 3.1e^{-3}$)	$r_s = 0.392$ ($p = 6.0e^{-4}$)

Spearman's Rho test; r_s-correlation coefficient. *In silico* analyses of tumor samples from 103 HPV^- HNC patients obtained from the TCGA data bank presented as r_s.

To further evaluate the probability of HLA-I/APM induction by T cell derived IFN-γ, basal and IFN- γ-regulated transcription and protein expression levels in three human HNSCC cell lines were determined using qPCR, Western blot analyses and flow cytometry. In this approach constitutive, but rather low mRNA levels of HLA-I APM components were detected in all three analyzed cell lines, which was even more pronounced at the protein level and accompanied by low HLA-I surface expression levels. IFN-γ treatment upregulated both HLA-I and APM mRNA and protein expression (Supplementary Figure 2A) suggesting a direct link between HLA-I/APM upregulation and T cell induced IFN-γ-secretion.

Preprints (www.preprints.org) | NOT PEER-REVIEWED | Posted: 10 September 2020 doi:10.20944/preprints202009.0238.v1

2.4 Impact of OSCC HLA-I/APM expression on the outcome of the patients

To elucidate the clinical impact of the different HLA-I/APM phenotypes of OSCC, the HLA-I APM expression results were set in relation to the OS of the patients using uni- and multivariable Cox proportional hazard regression and visualization by Kaplan-Meier curves. Here, an increase in HLA-I HC and β_2-m expression negatively affected the OS independent of the tumor size. We next analyzed whether this effect was influenced by the T stage or, more specifically, the tumor mass. When considering T1/2 vs. T3/4 tumors, no significant effect was found (Table 4A). In contrast, by solely focusing on T2 tumors, a significant worse OS and 4.4-fold higher risk of death (p=0.003; multivariable Cox regression, adjusting for UICC N-stage and grading) was detected in phenotype I [HLA-I^{high}/APM^{high}] in comparison to phenotype III [HLA-I$^{discordant\ low/high}$/APM^{high}] and to a lesser intent to phenotype II [HLA-I^{low}/APM^{low}] (Figure 2). Based on these data, we assume that the different results of T1 versus T2 tumors were due to the much better OS of patients with T1 tumors independent of the immune phenotype (Table 1).

In line with these data, *in silico* analyses employing the XENA database (https://xenabrowser.net/) revealed a reduced OS in HLA-I^{high}/APM^{high} HNSCC in comparison to HLA-I^{low}/APM^{low} HNSCC lesions. In this study, higher levels of TAP1 expression correlated with a better OS (Table 4B).

Table 4: Correlation of OSCC HLA-I/APM expression, T stage, intratumoral T cell infiltrate and overall survival

A: Expression of HLA-I/APM components and correlation with the T stage and overall survival

	no. of cases	overall survival (OS)					
		all tumors		T1-2 stage tumors		T3-4 stage tumors	
		univariable analysis	multivariable analysis*	no. of cases	multivariable analysis*	no. of cases	multivariable analysis*
		RR; p-value	RR; p-value		RR; p-value		RR; p-value
HLA-APM phenotype cytoplasmic and membranous							
I [HLA-I^{high}-APM^{high}]	57	I vs. III: 0.59; p=0.63	I vs. III: 1.29; p=0.55	31	I vs.III: 1.86 ; p=0.11	26	I vs. III: 1.08; p= 0.82
II [HLA-I^{low}-APM^{low}]	12			5		7	
III [HLA-I$^{high/low}$-APM^{high}]	89			43		46	
IV [HLA-I$^{high/low}$-APM^{low}]	2			2		0	

Preprints (www.preprints.org) | NOT PEER-REVIEWED | Posted: 10 September 2020 doi:10.20944/preprints202009.0238.v1

HLA-I HC							
cytoplasmic							
IRS 0-3	64			34		30	
IRS 4-12	96	1.53; p=0.07	1.52; p=0.08	51	1.86; p=0.11	49	1.25; p=0.47
membranous							
IRS 0-4	100			51		49	
IRS 6-12	60	1.13; p=0.59	1.04; p=0.86	30	1.85; p=0.10	30	0.72; p=0.26
β_2-m							
cytoplasmic							
IRS 0-3	48			27		21	
IRS 4-12	112	**1.80; p=0.026**	1.66; p=0.056	54	2.29; p=0.061	58	1.41; p=0.31
membranous							
IRS 0-4	105			56		53	
IRS 6-12	55	0.97; p=0.9	0.93; p=0.75	25	1.53; p=0.28	26	0.8; p=0.49
TAP1							
cytoplasmic							
IRS 0-2	18			8		10	
IRS 3-12	49	0.57; p=0.09	0.57; p=0.13	25	0.89; p=0.87	24	0.56; p=0.20
TAP2							
cytoplasmic							
IRS 0-4	49			26		23	
IRS 6-12	111	1.31; p=0.27	1.42; p=0.17	55	1.02; p=0.96	56	**2.35; p=0.02**
LMP2							
cytoplasmic							
IRS 0-4	105			53		52	
IRS 6-12	55	0.99; p=0.96	0.99; p=0.99	28	1.02; p=0.96	27	1.06; p=0.84
nuclear							
IRS 0-4	69			34		35	
IRS 6-12	91	1.52; p=0.07	1.56; p=0.054	47	**2.4; p=0.04**	44	1.44; p=0.2
LMP10							
cytoplasmic							
IRS 0-2	32			22		10	
IRS 3-12	128	1.54; p=0.15	1.27; p=0.43	59	1.34; p=0.5	69	1.33; p=0.51
nuclear							
IRS 0-4	21			12		9	
IRS 6-12	139	1.63; p=0.18	1.57; p=0.21	69	1.26; p=0.65	70	2.1; p=0.16

*Cox proportional hazards regression, adjusted for T, N stage and grading; RR, relative risk. Statistically significant data is marked in bold.

Preprints (www.preprints.org) | NOT PEER-REVIEWED | Posted: 10 September 2020 doi:10.20944/preprints202009.0238.v1

B: Correlation of OS to the HLA-I/APM component expression using TCGA data of 103 HPV$^-$ HNC patients

high HLA-A, HLA-B or β_2-m (phenotype I)	**TAP1**	**TAP2**	**LMP2**	**LMP10**
HLA-A	p = 0.028	p = 0.04	p = 0.068	p = 0.131
HLA-B	p = 0.479	p = 0.195	p = 0.045	p = 0.077
β_2-m	p = 0.019	p = 0.067	p = 0.074	p = 0.145
low HLA-A, HLA-B or β_2-m (phenotype II)	**TAP1**	**TAP2**	**LMP2**	**LMP10**
HLA-A	p = 0.679	p = 0.04	p = 0.059	p = 0.557
HLA-B	p = 0.884	p = 0.094	p = 0.028	p = 0.624
β_2-m	p = 0.873	p = 0.058	p = 0.055	p = 0.801

The expression data of HLA-I and APM components were obtained from the TCGA of 103 HPV$^-$ OSCC lesions. The mRNA expression patterns of the APM components TAP1, TAP2 and LMP7 within the in phenotype I and II were correlated to the OS of HPV$^-$ HNC patients. The red background in phenotype I indicates a lower OS when TAP1, TAP2 and LMP2 genes and HLA-A, HLA-B and β_2-m are highly expressed ($p \leq 0.1$), while the grey background indicates no significant differences in the phenotype I. Low expression levels of TAP2, LMP2 and HLA in phenotype II were associated with a better OS (green background), while the grey background indicates no significant differences ($p \leq 0.1$).

Preprints (www.preprints.org) | NOT PEER-REVIEWED | Posted: 10 September 2020 doi:10.20944/preprints202009.0238.v1

Figure 2: Overall survival of OSCC patients depending on HLA-I / APM phenotype.

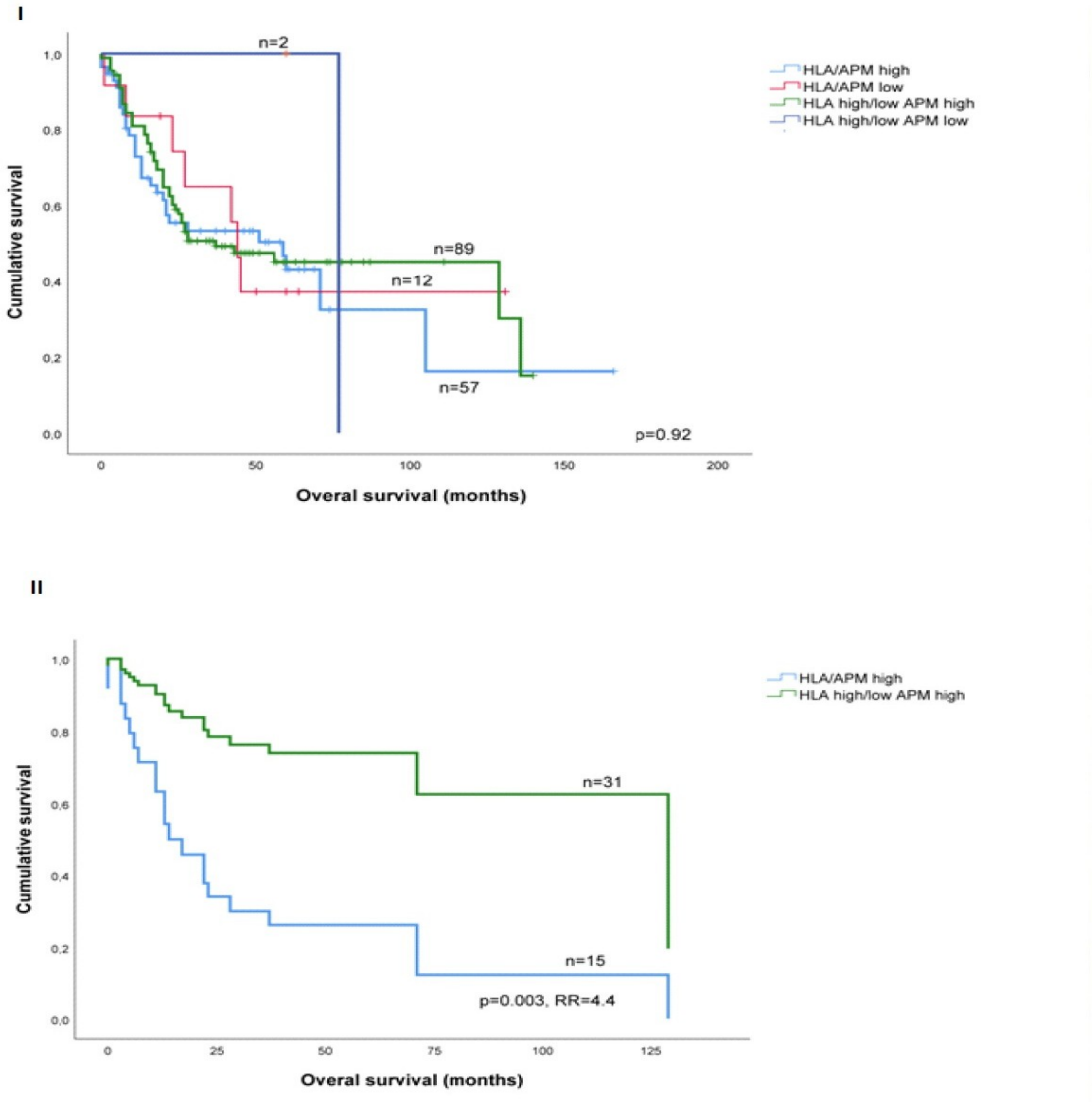

I: Comparison of OS of the four HLA-I/APM phenotypes irrespective of the tumor size. No clear separation of the survival curves was found.

II: OS of patients with T2 stage tumors. Selectively within this group patients with a HLA-I^{high}/APM^{high} phenotype had a 4.4-fold higher risk to die from OSCC when compared to patients with HLA-$I^{discordant\ high/low}$/APM^{high} and HLA-I^{low}/APM^{low} phenotype (multivariable Cox regression adjusting for UICC N stage as well as grading).

3. Discussion

Preprints (www.preprints.org) | NOT PEER-REVIEWED | Posted: 10 September 2020 doi:10.20944/preprints202009.0238.v1

It has become evident that an altered expression pattern of HLA-I antigens and HLA-I APM components in tumors represents an important immune escape mechanism from CTL-mediated elimination in distinct tumor types, which is frequently associated with poor prognosis and resistance to immunotherapy, and has been linked to changes in the TME [37-40]. In HNSCC, an immune suppressive equilibrium has been identified, which is characterized by a low frequency of dysfunctional immune effector cells and an altered expression of immune modulatory molecules of HNSCC cells [41]. In HPV^+ HNSCC, the distinct underlying immune escape mechanisms have been well identified [7, 42], while there is still a lack of data concerning immune evasion of HPV^- OSCC lesions. However, recent evidence suggested that the immune system plays an important role in the carcinogenesis of HNSCC independent of the HPV status. To get more insights into these processes, this study examined the expression and localization of HLA-I and APM components in HPV^- OSCC lesions and correlated the expression pattern with the frequency and density of the intratumoral immune cell infiltrate and clinical parameters to identify prognostic markers of OSCC progression and regulatory pathways, which can be potentially useful in the therapeutic setting. Impaired expression of HLA-I APM components is a frequent event in solid tumors when compared to non-malignant cells thereby progressively inhibiting the ability of $CD8^+$ CTL to recognize tumor cells [7, 38, 43-45]. Indeed, in the panel of HPV^- OSCC lesions analyzed in this study an impaired HLA-I APM expression was detected when compared to adjacent non-tumorigenic tissues, which was more prominent for HLA_I HC and b2-m than for the peptide transporters and proteasome subunits. Since this effect significantly varied between the OSCC lesions, the tumors were classified into three major phenotypes according to their HLA-I APM component expression ($HLA\text{-}I^{high}/APM^{high}$, $HLA\text{-}I^{low}/APM^{low}$, $HLA\text{-}I^{discordant\ high/low}/APM^{high}$). These groups were equally distributed within the different T stages, but were associated with a distinct TME regarding the type, density and spatial distribution of infiltrating immune cells. As expected, a correlation of HLA-I/APM expression with the immune cell infiltrate demonstrated a direct link of high intratumoral $CD8^+$ T cell infiltration with high levels of HLA-I APM component and HLA-I surface expression. To get insight whether HLA-I APM component expression and T cell infiltrate could be functionally connected, HNSCC cell lines were analyzed for their basal and IFN-γ induced expression. As low levels of HLA-I APM component expression in HNSCC cell lines were enhanced upon IFN-γ treatment, we suggest that a deregulation rather than structural alterations of these molecules might be responsible for the altered HLA-I/APM component expression in OSCC tumors. Furthermore, the concordance between HLA-I/APM expression and the frequency of $CD8^+$ T cells might be linked to IFN-γ secreted by immune cells, known to revert HLA-I downregulation [5]. In this context, it is important to consider that a striking difference between the HLA-I/APM phenotypes was obvious for the FOXP3:CD8 ratio, which was more than threefold higher in phenotypes II and III compared to phenotype I.

Thus, our experimental data suggest that the immunological control of phenotype I tumors might be associated with patients´ outcome. Unexpectedly, the correlation of the HLA-I/APM phenotypes to clinical data revealed that the HLA-I^{high}/APM^{high} subgroup despite a high intratumoral CD8$^+$ frequency and a rather low FOXP3:CD8$^+$ ratio was linked to an adverse outcome, which was most significant in T2 disease, while due to their excellent prognosis, this effect was not detected in T1 tumors. This is in line with a number of studies demonstrating at least for high levels of β_2-m a correlation with a poor prognosis [46, 47]. Furthermore, experimental models suggest that β_2-m overexpression is associated with a poor survival due to increased migration and invasion of OSCC cells [48].These data considerably extend our knowledge concerning the prognostic value of different components of the immune cell infiltrate. In this context, it is important to mention that next to melanoma, non-small cell lung cancer and CRC, in which a relationship between immune cell activity, HLA-I antigens, clinical outcome as well as response to CPI has been proven [18, 37, 49], our group recently showed a significant prognostic value of the presence and quantity of tumor infiltrating lymphocytes (TIL) in OSCC [32]. Taken the data of this study into account the established, prognostic relevant immune suppression index including the parameters CD8, FOXP3 distance to CD8 and PD-L1 expression has to be extended at least by the factor HLA-I expression, since a significant adverse outcome in tumors with a HLA-I^{high}/APM^{high} phenotype and high intratumoral CD8$^+$ cell content was found.

Assuming that the high levels of HLA-I HC and β_2-m in the phenotype I OSCC tumors might be often due to the IFN-γ secretion of T cells, an explanation for the adverse patients´ outcome might be caused by a systemic exhaustion leading to dysfunctional T cells both in blood and in the TME as described by others [50]. It is noteworthy that in our study the functionality of intratumoral T cells was not analyzed, since this study focused on the HLA-I/APM expression pattern. In contrast to the general dogma, patients with a HLA-I$^{discordant\ high/low}$ phenotype had a significant better prognosis compared to the HLA-I^{high} phenotype, which is in line with a report in CRC, in which HLA-A2-positive patients had a poorer tumor differentiation [51]. However, most important finding in this context is limited (T1/T2) tumor disease suggesting that the tumor burden might play a key role in the stage dependent immunological control of OSCC. In conclusion, we state that a multifactorial tumor protecting microenvironment rather than a reduced HLA-I/APM expression determines the outcome of OSCC especially in early T stages of this disease. This assumption is underlined by a recent study showing a significant correlation between the frequency of CD90$^+$ mesenchymal stem cells with tumor size in HNSCC [52].

These data conclusively emphasize an influence of a plethora of other factors or immune cells in the OSCC patients´ responses to immunotherapy, since neither the intratumoral CD8$^+$ cell

 doi:10.20944/preprints202009.0238.v1

content nor the downregulation of HLA-I alone predict therapy success especially in limited tumor disease.

Preprints (www.preprints.org) | NOT PEER-REVIEWED | Posted: 10 September 2020 doi:10.20944/preprints202009.0238.v1

4. Materials and methods

4.1 Basic patient's characteristics, inclusion criteria and study approval

The basal patient`s cohort consists of 246 consecutive untreated OSCC patients who either had the initial biopsy and / or were treated with surgery at the Department of Oral and Maxillofacial Surgery, University Hospital Halle (Saale), Germany collected between 1995 and 2014. The cohort underwent surgical procedure and in all cases, the resection of the primary OSCC was done in combination with a neck dissection. Here, ipsilateral to the site of primary tumor levels 1 – 5 were dissected, contralateral the levels 1 and 2. The resection margins were 1 cm in all dimensions. Dependent on UICC stage an adjuvant radio-/radiochemotherapy was added.

The study was carried out in compliance with the Helsinki Declaration and was approved by the Ethics Committee of the Medical Faculty of the Martin Luther University Halle-Wittenberg (study # 2017-81 and 2020-103). All cases had written consensus of patients. 72 cases were omitted from the study due to the dimension of suitable FFPE tissue or to insufficient tissue quality. All remaining tissue samples were tested for HPV association by either p16 IHC (Zeta Corp., Clone G175-405, dilution 1:25) and/or HPV PCR (Zytovision HPV Chip 1.0). 17 patients were omitted from the study because of a positive HPV status resulting in 160 cases for analyses.

With latest update of the cohort on July 1st 2020, after a median follow-up time of 27 months, 53% of the cohort (85 patients) had deceased with a median survival time at 22 months (mean 16 months). The basic clinical and histopathological data, therapeutic regimens and their association with OS were summarized in Table 1A and 1B. The tumors were classified as T stage 1 (n=32; 20%), 2 (49; 31%), 3 (24; 15%) and 4 (55; 34%) with and without nodal or distant metastasis.

4.2 Standard and multiplex immunohistochemistry

Immunohistochemical analyses of tissue samples were performed as recently described [32]. Briefly, FFPE tissue probes were incubated with the following primary mAbs: NAMB (β_2-m; SP09-36; dilution 1:50), HC10 (against free HC of HLA-B and -C molecules; HSP09-35; 1:2500), NOB1 (TAP1; SP12-156; 1:50), NOB2 (TAP2; SP12-157; 1:50), SY-1 (LMP2; SP08-118; 1:200) and TO-7 (LMP10; SP08-225; 1:200). To determine, whether biologically active (β_2-m-bound) HLA-A/B/C complex was expressed on OSCC, we performed IHC on fresh frozen tumor tissues of 10 exemplary cases was performed using the W6/32 mAb recognizing the HLA-A, -B and -C HC/β_2-m antigen complex (dilution 1:10) [36]. After fixation with formalin for 3 minutes followed by a washing step the specimen were incubated with the primary antibody for 30 minutes, a post-block reagent for 20 minutes and a HRP polymer for 30 minutes all at

room temperature with a washing step in between. Visualization was done with DAB and hemalaun as described above.

Immunohistochemistry (IHC) results were semi-quantitatively evaluated utilizing the immune reactive score (IRS) as described by Remmele *et al.* [35]. In short, for evaluation of membranous, cytoplasmic and nuclear staining intensity (0-negative, 1-low, 2-moderate, 3-strong positive) as well as percentage of stained cells (0-negative, 1- <10%, 2- 10-50%, 3- 51-80%, 4- >80%) were evaluated and the IRS then calculated as the product of both ranging from 0-12. .Ten percent of all cases plus all cases presenting any technical challenges were independently evaluated by two pathologists (CW, DB) and co-reviewed to harmonize and ensure reproducibility of the scoring. One pathologist (DB) scored all the remaining cases.

For correlation analyses of the expression of HLA-I and APM components with the frequency and localization of immune cell subpopulations within the tumor, multispectral imaging data from the same patient cohort (n=108 with immune cell data) previously published by us were employed [32].

4.3. Definition of the HLA-I/APM phenotypes

Based on the HLA-I (HC/β_2-m) and APM (TAP, LMP) component expression pattern, OSCC were categorized into four distinct HLA/APM phenotypes. In detail, based on the median IRS of membranous HLA-I HC and β_2-m expression, HLA expression was dichotomized in “HLA-I high” (median ≥ 4) and “HLA-I low” (median ≤ 3). Based on the median IRS of cytoplasmic TAP1 and TAP2 as well as the median IRS of nuclear LMP2 and LMP10, APM expression was dichotomized in “APM high” (median ≥ 4) and “APM low” (median ≤ 3). As a consequence, four distinct phenotypes (I-IV) could be defined: (i) phenotype I expressed high levels of both the HLA-I HC/β_2-m and APM components (“**HLA-I^{high}/APM^{high}**”), (ii) phenotype II displayed a low expression pattern of both HC/β_2-m and APM components (“**HLA-I^{low}/APM^{low}**”), (iii) phenotype III expressed discordant levels of HLA-I HC/β_2-m (HLA$^{high/low}$ or HLA$^{low/high}$) and high levels of APM components (“**HLA-I$^{discordant\ high/low}$/APM^{high}**”) and phenotype IV displayed discordant levels of HLA-I HC/β_2-m (HLA$^{high/low}$ or HLA$^{low/high}$) and low APM levels (“**HLA-I$^{discordant\ high/low}$/APM^{low}**”).

4.4 Bioinformatics

In silico analysis was performed using the R2 web tool (http://r2.amc.nl) in order to predict the correlation of HLA-I APM components, CD4, CD8, CD274 and FoxP3 with the mRNA expression of the different genes in HPV$^-$ head and neck cancer (HNC) patients. For this, the TCGA data set “Tumor head and neck squamous cell carcinoma” was chosen (n=520). HPV$^+$ HNC patients and patients with unknown HPV status were omitted from the calculations, while HPV$^-$ HNC patients (hpv_status_p16-negative, 103 patients) with data available for the

Preprints (www.preprints.org) | NOT PEER-REVIEWED | Posted: 10 September 2020 doi:10.20944/preprints202009.0238.v1

respective markers were analyzed. The 2log expression ratio was compared and a linear regression was calculated. A p-value < $1e^{-3}$ was considered as significant.
For the OS analyses, the XENA database (https://xenabrowser.net) was employed for the TCGA Head and Neck Cancer study (n=604). Only primary tumor samples from HPV^- patients (hpv_status_p16-negative, 103 patients) were included. A p-value < 0.1 was considered as significant.

4.5 Statistical analyses

To evaluate the relationship between HLA-I/APM expression, tumor stage and outcome two groups (low vs. high protein expression levels) were selected for each marker based on an even distribution of patient numbers in these groups. Cox's regression hazard model and Kaplan-Meier analyses were used to estimate a correlation of HLA-I and APM expression with OS of OSCC patients. The Cox model was adjusted for prognostic effect of co-variables (T stage, N stage and grading), and relative risk (RR) was calculated. The OS was calculated from the day of histological tumor diagnosis until the date of last follow-up or (if applicable) death. The interrelationships between the different HLA-I antigens and APM components were tested with the Spearman's rank correlation (r_s, correlation coefficient). A probability (*p) of* <0.05 was defined as a significant result and marked with a star (or if lower than 0.01 with two stars). If not otherwise specified, the results from the cell culture experiments were expressed as mean of at least three biological replicates including standard deviation. All statistical analyses were performed using SPSS software version 20.0 (SPSS Inc., Chicago, USA) and Microsoft Excel 2010 (Microsoft Corporation). For the t-test, two samples assuming unequal variances have been selected.

4.6 *In vitro* induction of HLA-I/APM expression

For determination of the constitutive and IFN-γ inducible HLA-I/APM expression *in vitro*, the human head and neck squamous cell carcinoma (HNSCC) cell lines SAS, Cal33 and FaDu were cultured in RPMI medium supplemented with 10 % (v/v) fetal calf serum (PAN, Germany), 2 mM L-glutamine, 100 units/ml penicillin, and 100 µg/ml streptomycin at 37 °C in 5% (v/v) CO_2 humidified air and were left untreated or treated for 24 or 48 hrs with recombinant interferon (IFN)-γ (200 µg/ml). Analysis was performed either directly or employing cell pellets, stored in liquid nitrogen until further use.

4.7 RNA isolation, semi-quantitative and quantitative PCR

For evaluation of HLA-I/APM expression by the tumor cell lines as well as by a subcollective of OSCC with availability of FFPE and fresh frozen sections and specimen of normal oral

Preprints (www.preprints.org) | NOT PEER-REVIEWED | Posted: 10 September 2020 doi:10.20944/preprints202009.0238.v1

mucosa total RNA was extracted using the NucleoSpin RNA extraction kit (Macherey-Nagel) according to the manufacturer's instructions and converted to cDNA using the cDNA synthesis kit and oligo-dT primer from Thermo Scientific. Target-specific primers (Supplementary Table 2) have been already described [8]. PCR was performed in a Rotorgene and using the Rotorgene 6000™ series software (Qiagen, Hilden, Germany) using GAPDH as control and for normalization.

cDNA was synthesized from double DNase I digested total RNA (500 ng) using RevertAid™ H Minus First Strand cDNA synthesis kit (Fermentas, St. Ingbert, Germany). Thereafter, qRT-PCR was performed on Rotorgene 6000 (Qiagen) with a two-step protocol (40 cycles; 95 °C, 15 s; 60 °C, 30 s) using target-specific primers in combination with Platinum® SYBR® Green qPCR SuperMix-UDG (Invitrogen, Karlsruhe, Germany). Relative mRNA expression levels for specific genes were normalized to that of the housekeeping gene delta-aminolevulinate synthase (ALAS) 1. For determination the IFN-γ inducibility, the mRNA levels of untreated HNSCC cell lines were set to one and differences to expression levels of IFN-γ-treated cells were calculated. qPCR analyses were performed on samples obtained from three independent experiments.

4.8 Western blot analyses

Proteins were extracted from 1 × 10^7 cells from the three HNSCC cell lines and protein concentration was determined with the Pierce BCA protein assay kit (Fisher Scientific, Schwerte, Germany). For Western blot analyses, 50 µg protein/lane was separated on 8%-12% SDS-PAGEs, transferred onto nitrocellulose membranes (Schleicher & Schuell, Dassel, Germany), and stained with (3%, w/v) Ponceau S. Immunodetection was performed with specific primary mAbs directed against TAP1, TAP2, LMP2, LMP10, HLA-I HC and β_2-m (kindly provided by S. Ferrone, Harvard, Boston, USA) as recently described [8]. Staining of blots with a GAPDH mAb (Cell Signaling, Frankfurt, Germany) served as loading control. As secondary antibodies the horseradish peroxidase (HRP)-conjugated anti-rabbit and anti-mouse antibodies (DAKO, Hamburg, Germany), respectively, were used and the LumiLight WB substrate (Roche Diagnostics, Mannheim, Germany) was employed for detection and visualization with a CCD camera (Eastman Kodak Co., Berlin, Germany).

4.9 Flow cytometry

Flow cytometric analyses were performed on a BD LSRFortessa unit (Becton Dickinson, Biosciences, Heidelberg, Germany). Briefly, 5x10^5 cells left untreated or treated with 200 units/ml of recombinant IFN-γ for 48 hrs were washed twice in PBS followed by direct staining with the fluorescein isothiocyanate (FITC)-labeled mouse anti-human HLA-I mAb (W6/32) and

 doi:10.20944/preprints202009.0238.v1

the respective isotype control (Beckman Coulter, Krefeld, Germany) and then measured on a flow cytometer. For data evaluation, the Kaluza software (Beckman Coulter) was applied. The results are expressed as mean specific fluorescence intensity (MFI) obtained from at least three independent experiments.

Preprints (www.preprints.org) | NOT PEER-REVIEWED | Posted: 10 September 2020 doi:10.20944/preprints202009.0238.v1

5. Conclusions

Immunotherapy is a promising tool for the treatment of different malignancies. However, the survival benefit is limited to a subset of patients. A better understanding of the complex interactions between tumor cells and the tumor microenvironment is urgently needed to improve overall response for cancer patients and improve prognosis towards long-term outcome under immunotherapy.

In this study, of the HLA-I and APM component expression was analyzed in a large cohort of OSCC tissues and correlated to the intratumoral immune cell infiltrate. These findings were associated to the clinical data of the patients. Unexpectedly, despite a high intratumoral $CD8^+$ T cell content, tumors with high expression levels of HLA-I and APM components presented a rather unfavorable outcome, which was most significant in smaller (T1/T2) tumors. We conclude that an effective immunomodulatory treatment strategy in OSCC has to include the blockade of more than one immune regulatory axis.

Preprints (www.preprints.org) | NOT PEER-REVIEWED | Posted: 10 September 2020 doi:10.20944/preprints202009.0238.v1

6. Supplementary Material

Supplementary Table 1: Concordant membranous HLA-I HC and β_2-m expression with HLA-I surface expression in FFPE vs. frozen OSCC lesions

cases	FFPE specimen		fresh frozen specimen
	HC: IRS	β_2-m: IRS	HLA-A/B/C: IRS
high membranous HLA expression			
Case # 47	9	6	8
Case # 53	9	6	6
Case # 64	8	6	8
Case # 100	8	8	8
Case # 263	8	8	8
low / negative membranous HLA expression			
Case # 136	0	0	1
Case # 148	0	1	0
Case # 151	0	1	0
Case # 182	0	2	3
Case # 202	0	2	2

IRS: immune reactive score.

Staining patterns of HLA-I HC and β_2-m on FFPE specimen with known HLA expression status (concordant membranous positivity) were compared to HLA-I surface expression on fresh frozen tissues using the W6/32 antibody recognizing the trimeric HLA-I complex.

Preprints (www.preprints.org) | NOT PEER-REVIEWED | Posted: 10 September 2020 doi:10.20944/preprints202009.0238.v1

Supplementary Table 2: Primers used for analyses of HLA-I and APM component expression

primer	sequence	Tm
TAP1 FWD*	GGA ATC TCT GGC AAA GTC CA	60° C
TAP1 REV**	TGG GTG AAC TGC ATC TGG TA	60° C
TAP2 FWD	CCA AGA CGT CTC CTT TGC AT	60° C
TAP2 REV	TTC ATC CAG CAG CAC CTG TC	60° C
β_2-m FWD	CTC GCG CTA CTC TCT CTT	60° C
β_2-m REV	AAG ACC AGT CCT TGC TGA	60° C
HLA-A, -B, -C FWD	GCC TAC CAC GGC AAG GAT TAC	60° C
HLA-A, -B, -C REV	GGT GGC CTC ATG GTC AGA GA	60° C
LMP2 FWD	TGC TGC ATC CAC ATA ACC AT	60° C
LMP2 REV	TGT GCA CTC TCT GGT TCA GC	60° C
LMP10 FWD	GGG CTT CTC CTT CGA GAA CT	60° C
LMP10 REV	CAG CCC CAC AGC AGT AGA TT	60° C

*fwd = forward; **rev = reverse.

Preprints (www.preprints.org) | NOT PEER-REVIEWED | Posted: 10 September 2020 doi:10.20944/preprints202009.0238.v1

Supplementary Figure 1: *In silico* correlation of CD8 mRNA expression with HLA-A, β_2-m and APM components

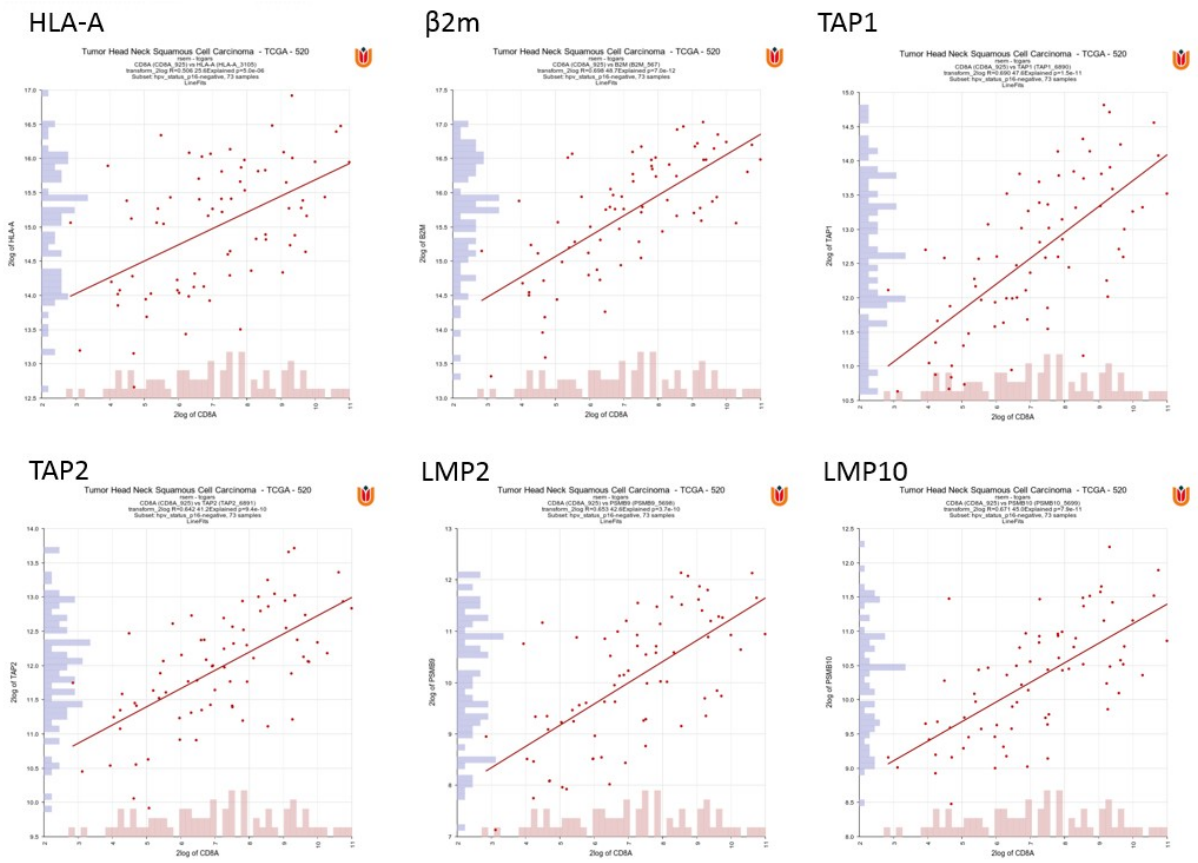

mRNA expression of CD8 was correlated with the mRNA expression of HLA-A, β_2-m, TAP1, TAP2, LMP2 and LMP10 in tumor material of HVP$^-$ HNSCC patients of the TCGA cohort (n=73). The histograms show the distribution of the patients as a xy-plot with the histogram and linear fit options. The p-value is given in the header of every histogram.

Preprints (www.preprints.org) | NOT PEER-REVIEWED | Posted: 10 September 2020 doi:10.20944/preprints202009.0238.v1

Supplementary Figure 2: Constitutive and IFN-γ mediated upregulation of HLA-I APM component expression in HNSCC cell lines.

A Effect of IFN-γ treatment on mRNA expression of HNSCC cell lines

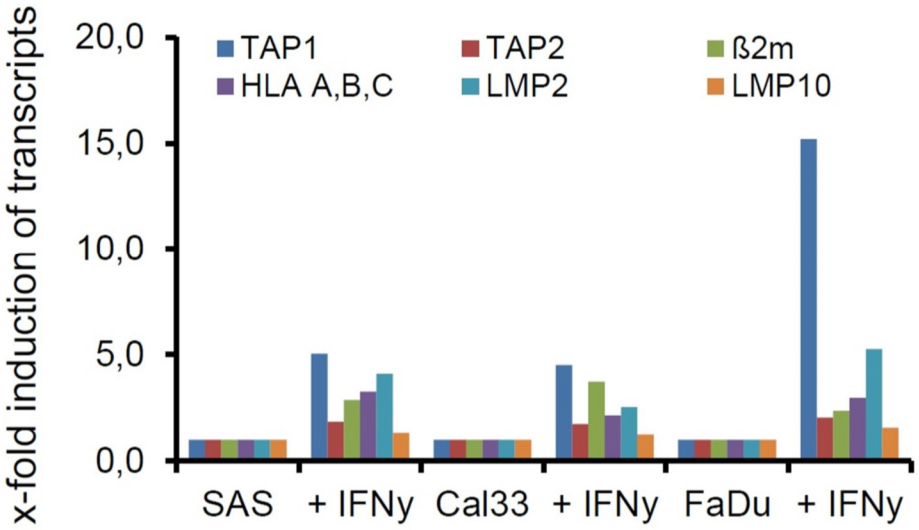

Ct value of APM component transcription

	SAS	SAS+IFNy	Cal33	Cal33+IFNy	FaDu	FaDu+IFNy
ß2m	8	9	9	9	8	9
HLA A,B,C	5	7	7	8	7	8
TAP1	6	7	7	8	6	8
TAP2	5	5	5	6	4	5
LMP2	7	8	8	9	7	9
LMP10	5	5	5	6	4	6

Ct value	10-12	12-14	14-16	16-18	18-20	20-22	22-24	24-26	>26
	9	8	7	6	5	4	3	2	1

A: HNSCC cell lines were left untreated or treated for 48 h with IFN-γ (200 U/ml) as described in Materials and Methods before qPCR was performed. The data represent the relative mRNA expression levels of the different APM components normalized to that of the housekeeping gene ALAS1. The transcription levels of untreated HNSCC cell lines were set to one, and respective expression levels of IFN-γ-treated cells were calculated. Ct values of HLA-/APM component transcription and their classification are given.

Preprints (www.preprints.org) | NOT PEER-REVIEWED | Posted: 10 September 2020 doi:10.20944/preprints202009.0238.v1

B Effect of IFN-γ on protein expression of HNSCC cell lines

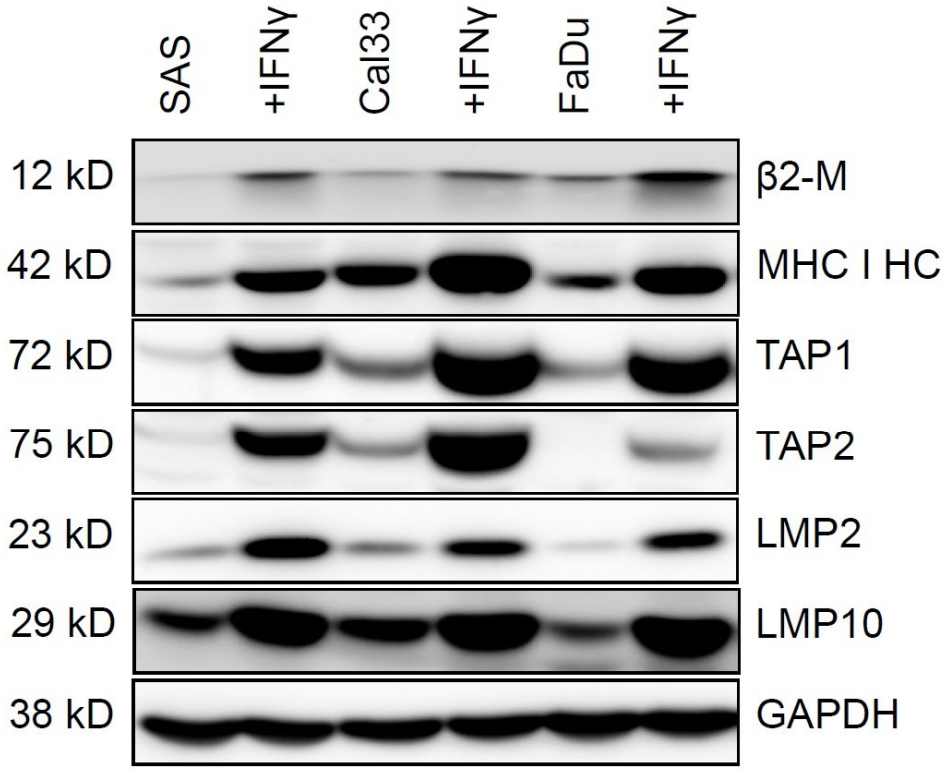

MHC class I surface expression as mean specific fluorescence intensity

Cell line	MFI (constitutive)	average deviation	MFI (IFN-γ)	average deviation
SAS	2.2	± 0.4	3.8	± 0.4
Cal33	3.5	± 0.8	6.9	± 1.7
FaDu	3.2	± 0.9	10.9	± 1.9

* mean of three independent replicates

B: Western blot analysis using 50 µg protein lysate/lane of three different HNSCC cell lines (SAS, Cal33, FaDu) left untreated or treated for 48 h with IFN-γ (200 U/ml) was performed as described in Materials and Methods. The detection of GAPDH served as loading control. HLA-I surface expression of untreated and IFN-γ-treated HNSCC cell lines was performed as described and data expressed as MFI.

Preprints (www.preprints.org) | NOT PEER-REVIEWED | Posted: 10 September 2020 doi:10.20944/preprints202009.0238.v1

7. Acknowledgements

We would like to thank Nicole Ott and Maria Heise from the Institute of Immunology for excellent secretarial help. Claudia Wickenhauser and Daniel Bethmann would like to thank the members of the Institute of Pathology`s, histology laboratory for their comprehensive help in this study.

8. Author's contributions

Barbara Seliger and Claudia Wickenhauser designed and supervised the project as well as analyzed and interpreted the results. Jana Beer and Daniel Bethmann performed the immunohistochemistry. Daniel Bethmann and Claudia Wickenhauser evaluated the immunohistochemistry. Jürgen Bukur performed the cell culture and flow cytometry experiments. Jürgen Bukur and Barbara Seliger evaluated the cell culture and flow cytometry experiments. André Steven performed the TCGA data acquisition and interpretation. Alexander Eckert and Matthias Kappler provided the fresh frozen OSCC samples and they collected the clinical data together with Daniel Bethmann. All authors participated in data analysis. Bernard Fox edited the manuscript, discussed the results and was involved in the MSI data generation and interpretation. Claudia Wickenhauser, Barbara Seliger and Daniel Bethmann drafted the manuscript.

9. Conflict of interest statement

BAF discloses consulting activities and/or research support related to multiplex IHC from Akoya Biosciences/PerkinElmer, Bristol-Myers Squibb, Definiens/AstraZeneca, Macrogenics, OncoSec and Ultivue. The remaining authors declare that there exist no conflicts of interest for any of the authors.

10. Ethics approval

The study was approved by the Ethics Committee of the Medical Faculty of the Martin Luther University Halle-Wittenberg, Halle, Germany (#2017-81).

11. Funding

This work was sponsored by the Deutsche Forschungsgemeinschaft project DFG 585/22-1 (BS) and the Mildred Scheel Foundation grants 110703 and 111091 (BS).

12. References

1. Tuccitto, A., et al., *Immunosuppressive circuits in tumor microenvironment and their influence on cancer treatment efficacy.* Virchows Arch, 2019. **474**(4): p. 407-420.
2. Draghi, A., et al., *Acquired resistance to cancer immunotherapy.* Semin Immunopathol, 2019. **41**(1): p. 31-40.
3. Kim, T.K., R.S. Herbst, and L. Chen, *Defining and Understanding Adaptive Resistance in Cancer Immunotherapy.* Trends Immunol, 2018. **39**(8): p. 624-631.
4. Fridman, W.H., et al., *The immune contexture in cancer prognosis and treatment.* Nat Rev Clin Oncol, 2017. **14**(12): p. 717-734.
5. Mandal, R., et al., *The head and neck cancer immune landscape and its immunotherapeutic implications.* JCI Insight, 2016. **1**(17): p. e89829.
6. Moy, J.D., J.M. Moskovitz, and R.L. Ferris, *Biological mechanisms of immune escape and implications for immunotherapy in head and neck squamous cell carcinoma.* Eur J Cancer, 2017. **76**: p. 152-166.
7. Concha-Benavente, F., et al., *Immunological and clinical significance of HLA class I antigen processing machinery component defects in malignant cells.* Oral Oncol, 2016. **58**: p. 52-8.
8. Respa, A., et al., *Association of IFN-gamma signal transduction defects with impaired HLA class I antigen processing in melanoma cell lines.* Clin Cancer Res, 2011. **17**(9): p. 2668-78.
9. Seliger, B., *Novel insights into the molecular mechanisms of HLA class I abnormalities.* Cancer Immunol Immunother, 2012. **61**(2): p. 249-254.
10. McGranahan, N., et al., *Allele-Specific HLA Loss and Immune Escape in Lung Cancer Evolution.* Cell, 2017. **171**(6): p. 1259-1271 e11.
11. Chowell, D., et al., *Patient HLA class I genotype influences cancer response to checkpoint blockade immunotherapy.* Science, 2018. **359**(6375): p. 582-587.
12. Shukla, S.A., et al., *Comprehensive analysis of cancer-associated somatic mutations in class I HLA genes.* Nat Biotechnol, 2015. **33**(11): p. 1152-8.
13. Eichmuller, S.B., et al., *Immune Modulatory microRNAs Involved in Tumor Attack and Tumor Immune Escape.* J Natl Cancer Inst, 2017. **109**(10).
14. Pages, F., et al., *International validation of the consensus Immunoscore for the classification of colon cancer: a prognostic and accuracy study.* Lancet, 2018. **391**(10135): p. 2128-2139.
15. Andersen, R., et al., *T-cell Responses in the Microenvironment of Primary Renal Cell Carcinoma-Implications for Adoptive Cell Therapy.* Cancer Immunol Res, 2018. **6**(2): p. 222-235.
16. Shin, D.S., et al., *Primary Resistance to PD-1 Blockade Mediated by JAK1/2 Mutations.* Cancer Discov, 2017. **7**(2): p. 188-201.
17. Zaretsky, J.M., et al., *Mutations Associated with Acquired Resistance to PD-1 Blockade in Melanoma.* N Engl J Med, 2016. **375**(9): p. 819-29.
18. Perea, F., et al., *The absence of HLA class I expression in non-small cell lung cancer correlates with the tumor tissue structure and the pattern of T cell infiltration.* Int J Cancer, 2017. **140**(4): p. 888-899.
19. Cohen, E.E.W., et al., *The Society for Immunotherapy of Cancer consensus statement on immunotherapy for the treatment of squamous cell carcinoma of the head and neck (HNSCC).* J Immunother Cancer, 2019. **7**(1): p. 184.
20. Pulte, D. and H. Brenner, *Changes in survival in head and neck cancers in the late 20th and early 21st century: a period analysis.* Oncologist, 2010. **15**(9): p. 994-1001.

21. Zini, A., R. Czerninski, and H.D. Sgan-Cohen, *Oral cancer over four decades: epidemiology, trends, histology, and survival by anatomical sites.* J Oral Pathol Med, 2010. **39**(4): p. 299-305.
22. Husain, N. and A. Neyaz, *Human papillomavirus associated head and neck squamous cell carcinoma: Controversies and new concepts.* J Oral Biol Craniofac Res, 2017. **7**(3): p. 198-205.
23. Omura, K., *Current status of oral cancer treatment strategies: surgical treatments for oral squamous cell carcinoma.* Int J Clin Oncol, 2014. **19**(3): p. 423-30.
24. Chow, L.Q.M., et al., *Antitumor Activity of Pembrolizumab in Biomarker-Unselected Patients With Recurrent and/or Metastatic Head and Neck Squamous Cell Carcinoma: Results From the Phase Ib KEYNOTE-012 Expansion Cohort.* J Clin Oncol, 2016. **34**(32): p. 3838-3845.
25. Ferris, R.L., et al., *Nivolumab in Patients With Recurrent or Metastatic Squamous Cell Carcinoma of the Head and Neck: Efficacy and Safety in CheckMate 141 by Prior Cetuximab Use.* Clin Cancer Res, 2019.
26. Haddad, R., et al., *Nivolumab treatment beyond RECIST-defined progression in recurrent or metastatic squamous cell carcinoma of the head and neck in CheckMate 141: A subgroup analysis of a randomized phase 3 clinical trial.* Cancer, 2019.
27. Cavalieri, S., et al., *Immuno-oncology in head and neck squamous cell cancers: News from clinical trials, emerging predictive factors and unmet needs.* Cancer Treat Rev, 2018. **65**: p. 78-86.
28. Foy, J.P., et al., *The immune microenvironment of HPV-negative oral squamous cell carcinoma from never-smokers and never-drinkers patients suggests higher clinical benefit of IDO1 and PD1/PD-L1 blockade.* Ann Oncol, 2017. **28**(8): p. 1934-1941.
29. Galon, J., et al., *Type, density, and location of immune cells within human colorectal tumors predict clinical outcome.* Science, 2006. **313**(5795): p. 1960-4.
30. Mlecnik, B., et al., *Integrative Analyses of Colorectal Cancer Show Immunoscore Is a Stronger Predictor of Patient Survival Than Microsatellite Instability.* Immunity, 2016. **44**(3): p. 698-711.
31. Herbst, R.S., et al., *Predictive correlates of response to the anti-PD-L1 antibody MPDL3280A in cancer patients.* Nature, 2014. **515**(7528): p. 563-7.
32. Feng, Z., et al., *Multiparametric immune profiling in HPV- oral squamous cell cancer.* JCI Insight, 2017. **2**(14).
33. Horton, J.D., et al., *Immune Evasion by Head and Neck Cancer: Foundations for Combination Therapy.* Trends Cancer, 2019. **5**(4): p. 208-232.
34. Muller, S., *Update from the 4th Edition of the World Health Organization of Head and Neck Tumours: Tumours of the Oral Cavity and Mobile Tongue.* Head Neck Pathol, 2017. **11**(1): p. 33-40.
35. Remmele, W. and H.E. Stegner, *[Recommendation for uniform definition of an immunoreactive score (IRS) for immunohistochemical estrogen receptor detection (ER-ICA) in breast cancer tissue].* Pathologe, 1987. **8**(3): p. 138-40.
36. Stam, N.J., et al., *HLA-A- and HLA-B-specific monoclonal antibodies reactive with free heavy chains in western blots, in formalin-fixed, paraffin-embedded tissue sections and in cryo-immuno-electron microscopy.* Int Immunol, 1990. **2**(2): p. 113-25.
37. Smyth, M.J., et al., *Combination cancer immunotherapies tailored to the tumour microenvironment.* Nat Rev Clin Oncol, 2016. **13**(3): p. 143-58.
38. Aptsiauri, N., F. Ruiz-Cabello, and F. Garrido, *The transition from HLA-I positive to HLA-I negative primary tumors: the road to escape from T-cell responses.* Curr Opin Immunol, 2018. **51**: p. 123-132.
39. Paulson, K.G., et al., *Acquired cancer resistance to combination immunotherapy from transcriptional loss of class I HLA.* Nat Commun, 2018. **9**(1): p. 3868.

40. Seliger, B., *Molecular mechanisms of HLA class I-mediated immune evasion of human tumors and their role in resistance to immunotherapies.* HLA, 2016. **88**(5): p. 213-220.
41. Botticelli, A., et al., *The 5-Ws of immunotherapy in head and neck cancer.* Crit Rev Oncol Hematol, 2020. **153**: p. 103041.
42. Krishna, S., et al., *Human Papilloma Virus Specific Immunogenicity and Dysfunction of CD8(+) T Cells in Head and Neck Cancer.* Cancer Res, 2018. **78**(21): p. 6159-6170.
43. Gettinger, S., et al., *Impaired HLA Class I Antigen Processing and Presentation as a Mechanism of Acquired Resistance to Immune Checkpoint Inhibitors in Lung Cancer.* Cancer Discov, 2017. **7**(12): p. 1420-1435.
44. Cai, L., et al., *Defective HLA class I antigen processing machinery in cancer.* Cancer Immunol Immunother, 2018. **67**(6): p. 999-1009.
45. Spranger, S., et al., *Density of immunogenic antigens does not explain the presence or absence of the T-cell-inflamed tumor microenvironment in melanoma.* Proc Natl Acad Sci U S A, 2016. **113**(48): p. E7759-E7768.
46. Klein, T., et al., *Correlation between tumour and serum beta 2m expression in patients with breast cancer.* Eur J Immunogenet, 1996. **23**(6): p. 417-23.
47. Tsimberidou, A.M., et al., *The prognostic significance of serum beta2 microglobulin levels in acute myeloid leukemia and prognostic scores predicting survival: analysis of 1,180 patients.* Clin Cancer Res, 2008. **14**(3): p. 721-30.
48. Chen, C.H., et al., *Overexpression of beta2-microglobulin is associated with poor survival in patients with oral cavity squamous cell carcinoma and contributes to oral cancer cell migration and invasion.* Br J Cancer, 2008. **99**(9): p. 1453-61.
49. Restifo, N.P., M.J. Smyth, and A. Snyder, *Acquired resistance to immunotherapy and future challenges.* Nat Rev Cancer, 2016. **16**(2): p. 121-6.
50. Ludwig, S., et al., *Suppression of Lymphocyte Functions by Plasma Exosomes Correlates with Disease Activity in Patients with Head and Neck Cancer.* Clin Cancer Res, 2017. **23**(16): p. 4843-4854.
51. Kiewe, P., et al., *HLA-A2 expression, stage, and survival in colorectal cancer.* Int J Colorectal Dis, 2008. **23**(8): p. 767-72.
52. Liotta, F., et al., *Mesenchymal stem cells are enriched in head neck squamous cell carcinoma, correlates with tumour size and inhibit T-cell proliferation.* Br J Cancer, 2015. **112**(4): p. 745-54.